ELSEVIER

Polymer 41 (2000) 2795–2806

polymer

Pervaporation of water, hydrazine and monomethylhydrazine using ethylcellulose membranes ☆

R. Ravindra[a], S. Sridhar[b], A.A. Khan[b,*], A.K. Rao[c]

[a]*R&D, LG Polymers, Vishakapatnam 530 029, India*
[b]*Membrane Separations Group, Chemical Engineering Division, Indian Institute of Chemical Technology, Hyderabad 500 007, India*
[c]*Department of Polymer Science and Technology, S.K. University, Anantapur 515 003, India*

Received 21 July 1998; received in revised form 7 January 1999; accepted 28 June 1999

Abstract

Ethylcellulose membrane has been selected on the basis of Hansen's solubility parameter and Flory–Huggins interaction parameter for the enrichment of hydrazine and monomethylhydrazine (MMH) liquid propellants by pervaporation. An extensive study of the overall mass transfer resistance experienced by the permeants has been conducted. The resistance values were quantitatively estimated by changing the membrane thickness and calculating the corresponding flux. Due to its lower sorption, and fewer interactions, the membrane showed least desorption resistance towards water and thus it is permselective with respect to water. Results of pervaporation selectivity obtained in separation of water–hydrazine and water–MMH mixtures at azeotropic compositions have been correlated. Higher sorption of MMH and hydrazine did not result in preferential separation inspite of lower membrane resistance. Experimental results clearly showed that desorption resistance and diffusivity were predominant over the respective solubilities. To confirm the reasons for these phenomena, FTIR and DSC spectra of membranes soaked in pure hydrazine, MMH, water and hydrazine hydrate were compared.

Keywords: Ethylcellulose; Membrane resistance; Pervaporation

1. Introduction

Pervaporation (PV) is an economical separation technique compared to conventional separation methods such as distillation especially in separations involving azeotropes [1], isomers [2] and removal or recovery of trace substances [3]. Due to its good separation efficiency and flux rates, PV results in savings in energy costs, besides ensuring safety in operations. A number of industrial applications use this technique for the dehydration of alcohols [4,5], for separation of isomeric compounds [6,7], and for separation of mixtures of chlorinated solvents [8], ketones, esters [9] and saturated hydrocarbons [10]. The US Department of Energy identified "pervaporation membranes for organic–organic separations, and reverse osmosis oxidation resistance membranes", as two of their highest ranking research priorities [11].

In the PV process, the feed mixture is contacted with a non-porous permselective membrane and separation can be explained by the solution-diffusion mechanism which involves steps of sorption into, diffusion through and desorption from the membrane [12]. The first and the last steps are usually considered to be fast and to take place at equilibrium. Diffusion is a slower process. The membrane itself is in pseudo-equilibrium, i.e. the swollen upstream surface is in equilibrium with the feed liquid whereas the downstream surface is virtually dry due to the vacuum prevailing in the permeate chamber. In this state, it is unlikely to be at equilibrium with the gas/vapour present in the vicinity. For most of the work reported in the literature, the upstream resistance has been taken into account to calculate the overall rate of mass transfer, while the interface boundary layer resistance that exists between the membrane surface and the permeate side has been excluded [13–16].

There are many theories developed to understand pervaporation as a separation process. In general, it is believed that at low permeate pressures and with a membrane having sufficient thickness the permeability is mainly governed by diffusion through the membrane. This implies that permeability is independent of membrane thickness and flux is inversely proportional to the latter.

☆ IICT Communication no. 4215.

* Corresponding author. Tel.: +91-40-7173626; fax: +91-40-7173757.
E-mail address: aakhan@csiict.ren.nic.in (A.A. Khan).

0032-3861/00/$ - see front matter
PII: S0032-3861(99)00487-5

However, in 1993 Bode and his associates [17] reported that permeability decreased with decreasing membrane thickness in the permeation of pure water through polyether block amide. The reason for this anomalous behaviour was explained on the basis of the theory of "membrane resistance at permeate side", postulated by Cote and Lipski [14], which states that there may be a resistance to mass transfer at the permeate side at high permeate pressures, i.e. a film formed due to non-desorbed vapours of permeants adjacent to the downstream interface. Quantification of the state depends on permeate pressures, membrane–permeant interaction, membrane structure and others. Evapomeation, a modified form of pervaporation also exhibits non-equilibrium situations, in which the membrane resistance at feed and permeate sides result in a decrease of flux values. In this case, the vapours of feed liquid are in direct contact with the membrane.

The present investigation attempts to quantify and explain the anomalous decrease in overall mass transfer rate in terms of the resistance offered at the permeate side by hydrodynamic boundary layer. Experimentally determined flux values and interaction of permeant with polymer matrix as observed by the FTIR and DSC spectra have been used for substantiating the results.

2. Experimental

2.1. Materials

The polymer used in the study was ethylcellulose (EC), having 48–49% ethoxy content, purchased from Loba Chemie (Mumbai, India). Its M_n (63 156) and M_w (89 448) were determined by the GPC method using polystyrene as the standard. Toluene, a solvent for EC, was also purchased from Loba Chemie, India, and was used as received without any further purification. Hydrazine and MMH were supplied by VSSC (ISRO), Thiruvananthapuram, India. Double distilled deionised water was used in all the experiments.

2.2. Membrane preparation

A clear polymer solution (15 wt%) in toluene was used for casting membranes of the desired thickness on a clean glass plate. Solvent was initially evaporated at room temperature (30°C) for 10 h and then the plate was kept under vacuum at 60°C for complete removal of the residual solvent in the membrane. The thickness of the dry membrane was measured with a micrometer of ± 1 μm least count.

2.3. Polymer selection

Selection of polymers for the separation is based mainly on three important aspects: the polymer should have high chemical resistance (compatibility), sorption capacity and good mechanical strength in the solution. The polymer should also have good interaction preferably with one of the components of the mixture for effective separation.

In general, selection of polymers compatible with the feed mixtures to be separated is based on the Hansen solubility parameter (Δ) and the Flory–Huggins interaction parameter (χ). For the first parameter (Δ), the compatibility among water, and hydrazine or MMH, and polymer is indicated by the following relationship [18]:

$$\Delta = \sqrt{[(\delta_{d,i} - \delta_{d,2})^2 + (\delta_{p,i} - \delta_{p,2})^2 + (\delta_{h,i} - \delta_{h,2})^2]} \quad (1)$$

where δ_p, δ_d, and δ_h are the polar, dispersive, and hydrogen bonding contributions and Δ is the magnitude of the vectorial distance in the three-dimensional diagram of δ_p, δ_d, and δ_h on *x*-, *y*- and *z*-axis, respectively. In Eq. (1) '*i*' represents water or propellant and '2' represents the polymer. The greater the compatibility between any two components, the smaller the magnitude of Δ.

The Flory–Huggins interaction parameter (χ) also signifies the compatibility of components with the polymer. The binary interaction parameters, $\chi_{1,3}$ and $\chi_{2,3}$ between the liquid species and the polymer can be determined from [19]:

$$\chi_{i,2} = \frac{[\ln(1 - V_P) + V_P]}{V_P^2} \quad (2)$$

where V_P is the volume fraction of polymer (2) and *i* stands for water, hydrazine or MMH. Again the smaller the value of χ (close to 0.5 but not below), the greater will be the interaction between the polymer and the liquid species. Based on the above factors EC membrane was found to be the most suitable for the dehydration of hydrazine and MMH [20,21]. The present study has been carried out to understand the reasons for the membrane performance with respect to these liquids.

2.4. FTIR studies

The FTIR spectra of dry EC membrane, and films soaked to equilibrium in pure component hydrazine, MMH and water were obtained after removing the excess adhering liquid with tissue paper. Scanning was carried out immediately using a Nicolet-740, Perkin–Elmer 283B FTIR Spectrometer (USA).

2.5. DSC studies

DSC studies were performed on the EC membranes soaked in hydrazine, water and hydrazine hydrate with a Perkin–Elmer DSC-7 model instrument. Membranes having varied amounts of residual solvent were prepared by immersing a totally dry membrane in the solvent for different durations and then removing the excess solvent on the surface with a filter paper. DSC scans were taken at a temperature range of −60–25°C and at a heating rate of 5°C/min.

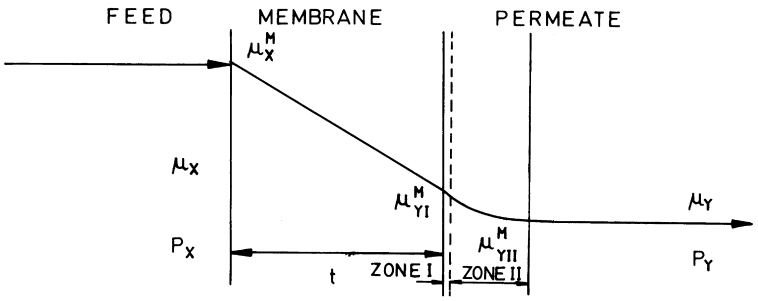

Fig. 1. Resistance model across the membrane.

3. Mass transfer through membrane

The permeation of a liquid through a membrane experiences two types of resistance, namely: (i) membrane interface resistance at the permeate side due to interaction of the permeant with the membrane material; and (ii) desorption resistance adjacent to the membrane due to the boundary layer on the permeant side.

The overall chemical potential profile of the permeant(s) across the system is simplified in Fig. 1 where μ, P and T represent the chemical potential, pressures and temperatures at feed (X), and permeate (Y) sides of the membrane (M).

On the basis of published results [14,15,17], two possible zones for the desorption resistance have been taken into account (Fig. 1): Zone I is the desorption interface [15,17], and Zone II is the boundary layer adjacent to the downstream interface of the membrane [14]. The resistance in Zone I is due to the diffusion of permeant through the polymer matrix at the outer layers of the membrane. On the contrary, the resistance in Zone II is due to the formation of a hydrodynamic boundary layer adjacent to the membrane surface. The desorption resistance of Zone I is significant when the membrane thickness is smaller, whereas at higher permeate pressures Zone II plays an important role. With increasing permeate pressures the thickness of the boundary layer increases causing more significant mass transfer resistance adjacent to the membrane surface. When the permeate pressure is well below the saturated vapour pressure of the permeant, Zone II may not be important in calculating the desorption resistance [14].

The overall process flux (j) can be described as

$$j = \alpha_t(\mu_X - \mu_Y) \tag{3}$$

where α_t is the overall mass transfer coefficient of the membrane with thickness t. Since the membrane is in equilibrium and the exchange of permeant molecules with feed liquid is substantial, $\mu_X = \mu_X^M$. Now the flux through the membrane in terms of the chemical potential at constant temperature can be written as

$$j = -L_\mu\left(\frac{d_{\mu_X}}{d_{\mu YI}}\right) \tag{4}$$

where $-L_\mu$ is the phenomenological coefficient which is equivalent to the permeability coefficient. Hence the flux equation becomes

$$j = \frac{L_\mu}{t} = (\mu_X^M - \mu_{Y1}^M) \tag{5}$$

and the flux equation between Zones I and II can be written as

$$j = \alpha_d(\mu_{YI}^M - \mu_{YII}^M) \tag{6}$$

where α_d is the mass transfer coefficient in the desorption step. Rearranging Eqs. (3)–(6) the mass transfer resistance (reciprocal of mass transfer coefficient (α_t) can be written as

$$\frac{1}{\alpha_t} = \frac{t}{L_\mu} + \frac{1}{\alpha_d} \tag{7}$$

thus the mass transfer resistance can be considered as the sum of a membrane resistance (t/L_μ) and desorption resistance ($1/\alpha_d$).

Thermodynamic equations for chemical potential of the single component in each step correlate the mass transfer coefficient and the permeate pressure. The thermodynamic equations are derived based on the earlier assumptions as

$$\mu_X = \mu_X^M \text{ and } a_X = a_X^M = 1$$

which implies that

$$\mu_X = \mu_0 + RT \ln a_X + \int_{P^*}^{P_X} V_X \, dP$$
$$\mu_X = \mu_0 + V_X(P_X - P^*) \qquad \mu_X = \mu_X^M \tag{8}$$

where a_X and a_Y are, respectively, the activities of the permeant in feed and permeate, then

$$\mu_{YI}^M = \mu_0 = RT \ln a_{YI} + \int_{P^*}^{P_X} V_X \, dP \tag{9}$$

assuming that pressure in the membrane is constant at P_X.

In Zone II, because of the low pressure the vapour is considered to be an ideal gas, and hence the chemical

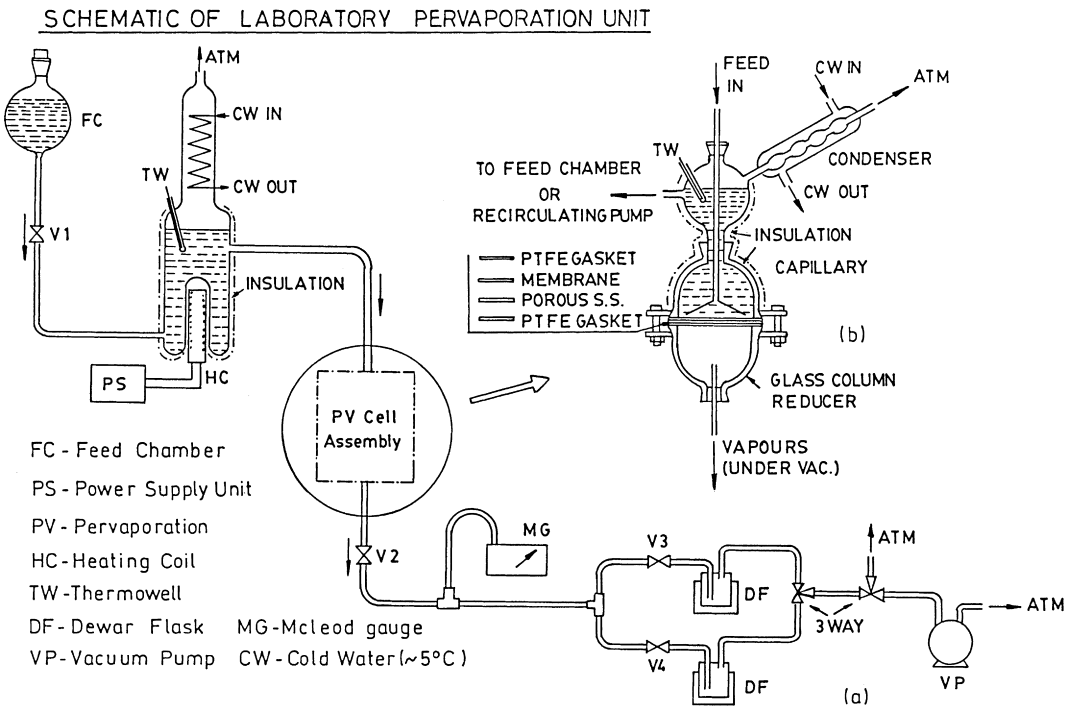

Fig. 2. Schematic of laboratory pervaporation unit.

potential equation can be written as

$$\mu_{\mathrm{YII}} = \mu_0 + \int_{P^*}^{P_\mathrm{Y}} V_\mathrm{Y}\,\mathrm{d}p$$
$$\mu_{\mathrm{YII}} = \mu_0 + \int_{P^*}^{P_\mathrm{Y}} \left(\frac{\mathrm{R}T}{P}\right)\mathrm{d}p = \mu_0 + \mathrm{R}T\ln\left(\frac{P^\mathrm{Y}}{P^*}\right) \tag{10}$$

where μ_0 and P^* are the chemical potential and saturation vapour pressure of the permeant, respectively, and V_Y is the molar volume of the permeant in permeate.

The overall chemical potential difference, $\Delta\mu$ is derived from Eqs. (8) and (10)

$$\Delta\mu = V_\mathrm{X}(P_\mathrm{X} - P^*) + \mathrm{R}T\ln\left(\frac{P^*}{P_\mathrm{Y}}\right). \tag{11}$$

By combining Eqs. (3) and (11), the overall mass transfer coefficient α_t can be obtained as

$$\alpha_t = \frac{j}{\mathrm{R}T\ln\left(\dfrac{P^*}{P_\mathrm{Y}}\right) + V(P_\mathrm{X} - P^*)} = \frac{j}{\Delta\mu} \tag{12}$$

Thus α_t can simply be determined from the measurement of the steady-state flux of the liquid species in pervaporation experiments and the saturation vapour pressure of permeants. Eq. (6) can be rewritten as

$$\frac{1}{\alpha_t} = \frac{\Delta\mu}{j} = \frac{t}{L_\mu} + \frac{1}{\alpha_\mathrm{d}}. \tag{13}$$

If the overall mass transfer resistance is plotted against the membrane thickness, a straight line is obtained for which the intercept is equal to the desorption resistance and the slope is equal to the membrane resistance.

In view of the above discussion, estimation of desorption resistance of the permeants across a membrane by pervaporation experiments is simplified. This can be achieved by measuring the fluxes of pure components, in this case water, hydrazine, MMH in EC membranes of thicknesses varying from 20 to 120 μm. By substituting the values of fluxes and vapour pressures of the permeants in the feed, permeate and also the saturation (P^*) state in Eq. (12), the overall mass transfer coefficient can be estimated. A graph plotted between membrane thickness and the corresponding coefficient of mass transfer resistance (inverse of mass transfer coefficient) results in a straight line. The slope of this line is the membrane resistance and the intercept is the desorption resistance of that particular liquid component for the boundary layer at the permeate side of the membrane.

3.1. Vapour pressure data

The vapour pressure data of pure hydrazine can be determined by using the equation formulated by Scott [22]:

$$\log p_{(\mathrm{mmHg})} = \frac{(7.80687 - 1680.745)}{(T + 227.74)} \tag{14}$$

where p is the vapour pressure at temperature T in degrees centigrade.

Vapour pressures of MMH based on data from Agarwal [23], and Aston [24] can be described by the following

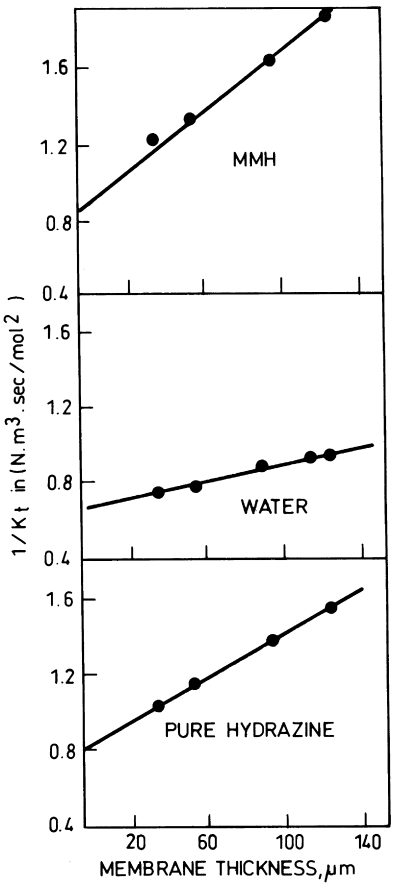

Fig. 3. Inverse overall mass transfer coefficient of pure liquids against membrane thickness through EC membrane at 25°C.

equation obtained from regression analysis of the data:

$$\log p_{(\mathrm{mmHg})} = 7.11158 - \left(\frac{1104.5711}{T}\right) - \left(\frac{152227.7}{T^2}\right) \tag{15}$$

where p is the vapour pressure of MMH at temperature T in Kelvin.

The above equation is valid between 265 and 360 K. The data between the boiling point and the critical point can be calculated by the following equation [24,25]:

$$\log p_{(\mathrm{atm})} = 4.5106 - \left(\frac{1355.07}{T}\right) - \left(\frac{98237.8}{T^2}\right). \tag{16}$$

Table 1
Parameters of ethylcellulose membrane resistance

	Water	Hydrazine	MMH
Desorption resistance (α_d)[a]	1.493×10^{12}	1.242×10^{14}	1.135×10^{13}
Membrane resistance (L_μ)[b]	0.588×10^{3}	0.180×10^{3}	0.132×10^{3}

[a] α_d in $\mathrm{mol^2\,N^{-1}\,m^{-3}\,s^{-1}}$.
[b] L_μ in $\mathrm{mol^2\,N^{-1}\,m^{-2}\,s^{-1}}$.

4. Pervaporation experiments

A schematic of the bench-scale PV unit is shown in Fig. 2. The membrane was supported by a stainless-steel screen embedded in a stainless-steel porous plate. The PTFE gaskets were fixed by means of high-vacuum silicone grease on either side of the membrane and the sandwich was placed between two glass column couplers and clamped together with external padded flanges by means of tie rods to give a vacuum-tight arrangement. The effective area of the membrane in the PV cell was 19.4 $\mathrm{cm^2}$. The top half was used as the feed chamber and the bottom half worked as the permeate chamber. At the beginning of each run, a dry membrane was mounted in the cell. Feed was introduced in the upper chamber and vacuum was applied from the opposite side. The permeate pressure was measured with an Edwards Mcleod gauge. Each experiment was repeated twice using fresh feed solution to check for reproducibility. The same volume of the feed material was introduced in each run to avoid any experimental disturbances. Pure component feeds were used for all the experiments and hence concentration polarisation was not expected to play any role.

Since pure MMH and hydrazine are highly hygroscopic in nature, effective sealing of the feed chamber was assured. All experiments were conducted at a feed temperature of 27 ± 1°C. The permeate pressure was maintained at 0.01 mmHg and permeate samples were collected in a cold trap (B) filled with a dry ice–acetone mixture after the membrane attained steady-state condition. The collected permeate was weighed after allowing it to attain room temperature and then analysed by an iodometric titration method [26].

5. Results and discussion

5.1. Pervaporation experimental results

The pervaporation experiments were repeated for different pure component feeds (water, hydrazine and MMH) with membranes of varying thicknesses (t) from 25 to 125 μm. Desorption resistance and membrane resistance for water, hydrazine and MMH in ethylcellulose membrane were estimated by recording the vapour pressures of the desired component in feed, permeate and at saturation state from Eqs. (14)–(16). Eq. (12) was used to determine the overall mass transfer coefficient (Section 3). For each feed component, a graph between the overall resistance $1/\alpha_t$ and membrane thickness was plotted on the y- and x-axes, respectively. The graphs for hydrazine, water and MMH are shown in Fig. 3(a)–(c), respectively. From each graph the values of the slope (membrane resistance) and intercept (desorption resistance) were obtained (Table 1).

Table 1 clearly indicates that the desorption resistance of hydrazine in EC is higher than that of water and MMH.

FTIR studies [26], DSC experiments [27] and sorption results (discussed in the forthcoming sections) suggest that the binding capacity of hydrazine with EC is higher than that of water and it also influences the functional groups of the ethylcellulose repeating unit to a greater extent than the other two liquids. This confirms that hydrazine has higher affinity towards EC and it binds well to the polymer matrix. Hence, higher energies are required to dislodge the hydrazine molecules from the polymer matrix and this offers higher desorption resistance. Similarly, MMH too showed a higher sorption value than water, and thus the membrane was found to possess higher desorption resistance towards MMH relative to water.

EC shows maximum membrane resistance towards water, when compared to pure hydrazine and MMH, which implies that the membrane has lower affinity for water and, hence, it contains a lower quantity of water at any time. Desorption resistance for water is lower and the diffusion coefficient is higher. These characteristics allow water molecules to move faster into the membrane and to leave the membrane without much resistance at the permeate side. Hydrazine and MMH have almost double the sorption values but because of their lower diffusivity values, their transfer rates are not as high as water molecules. Excessive interaction with the polymer matrix and higher desorption resistance result in higher retention time for these molecules compared to water in the membrane. FTIR and DSC studies, explained in the following sections, also indicate the retention of hydrazine molecules in the membrane matrix. Experimental results show that pure water fluxes are greater than hydrazine and MMH. A feed consisting of hydrates of hydrazine or MMH will result in a permeate containing more water thus proving that the membrane is selective with respect to water.

The weight percent sorption values of water, hydrazine and MMH with EC are 3.5, 7.5 and 15.5, respectively [26], clearly indicating that water has a smaller sorption value. Membrane resistances to hydrazine and MMH are almost similar. A slightly higher value of membrane resistance with MMH may be due to its larger molecular size compared to that of hydrazine.

The values of desorption resistance and diffusion coefficients [26] confirm the presence of larger amounts of water at the permeate side. These are the key factors in the separation of water from its mixtures with hydrazine or MMH.

5.2. Hansen and Flory–Huggins interaction parameters

Inserting the Hansen solubility parameter (δ) values [34,35] in Eq. (1), the Δ values for the permeant–EC systems were found to be 9.8, 16.0 and 30.0 for MMH, hydrazine and water, respectively. Similarly, the Flory–Huggins interaction parameters were equal to 1.39, 1.84 and 2.54 for EC–MMH, EC–hydrazine and EC–water systems, respectively. The values of the Δ and χ for EC–MMH and EC–hydrazine were very small compared to those obtained for the EC–water system. This could be the reason for the greater solubility of the liquid propellants in EC relative to water. Further, water is a smaller molecule compared to hydrazine and MMH. A similar example is the one involving ethanol–water separation [36] by hydrophobic PVC membrane, for which PVC had greater affinity and solubility for ethanol than water, whereas it showed greater overall diffusion selectivity with respect to water. The selectivity values obtained from diffusion and solubility studies were of a similar order of magnitude to those evaluated from pervaporation experiments for which the average selectivity values were equal to 2.3 and 5.6 with respect to water for the separation of hydrazine–water and MMH–water, respectively. This confirms the hypothesis that the propellants are more strongly held by polymer molecules, which results in their greater sorption, while water is less strongly held and is thus able to diffuse faster than MMH.

5.3. Membrane selectivity

The values of diffusion coefficients (D), calculated from reduced sorption curves [26,33] are 2.57×10^{-8}, 0.28×10^{-8} and 9.51×10^{-9} cm^2/s for water, hydrazine and MMH and the equilibrium percentage sorption were 3.4, 7.96 and 15.66, respectively, for the three liquids. Solubility coefficients (S) can be calculated by knowing the volume of penetrant observed per cm^3 of dry polymer, and dividing it by the vapour pressure of penetrant [34] at the temperature at which experiments were conducted. The values of S were calculated and found to be 1.13×10^{-3}, 4.71×10^{-3} and 3.89×10^{-3} (g/g)/mmHg for water, hydrazine and MMH, respectively. From the solubility and diffusion coefficients, the relative permeability or the overall selectivity were calculated by the following relation:

$$\text{Overall selectivity} = \left(\frac{S_{\text{water}}}{S_{\text{hydrazine/MMH}}}\right)\left(\frac{D_{\text{water}}}{D_{\text{hydrazine/MMH}}}\right). \tag{17}$$

The overall solubilities of water–hydrazine and water–MMH estimated from Eq. (17) are equal to 2.17 and 3.67, respectively. The selectivity values thus obtained give an approximate estimate as the above procedure is applicable only to cases where penetrant partial pressures are nearly the same as those in the experiments [20,21]. Further prediction of mixture selectivity based upon pure component sorption and diffusion curves can be used only as a guideline in cases where penetrants interact intensively with the polymer matrix. However, in this case it was confirmed that the EC membrane is more selective towards water, which has a higher diffusivity coefficient (and flux) compared to MMH and hydrazine.

5.4. FTIR interaction studies [26]

The FTIR spectrum of pure dry EC film is shown in Fig. 4. The peak at 3500 cm^{-1} is of –OH groups present on the

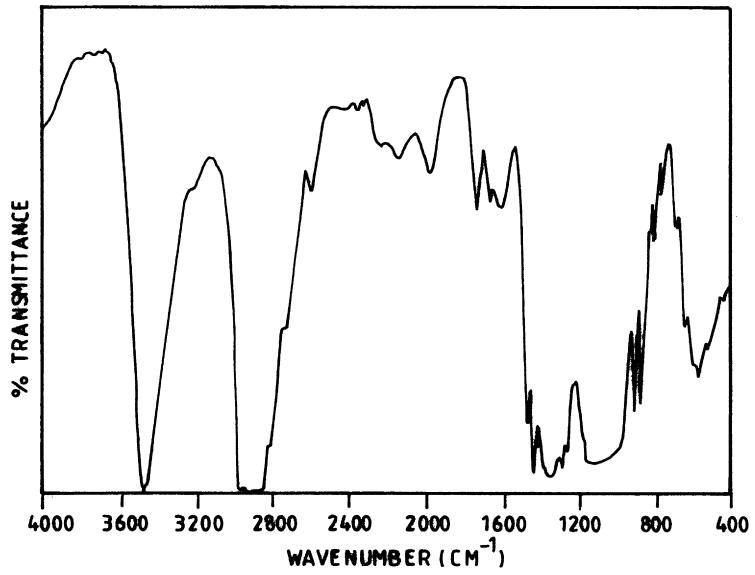

Fig. 4. FTIR spectrum of ethylcellulose membrane.

closed ring structure of the polymer repeating units. A shoulder peak at 3250 cm^{-1} corresponds to associated –OH of intermolecular bonding. The small but not sharp peak at $\approx$ 2950 cm^{-1} corresponds to asymmetric structure vibrations of the $-OC_2H_5$ ethoxy groups. There are small peaks between 2850 and 2720 cm^{-1} corresponding to –CHO stretching, which is sharp at 2650 cm^{-1}. The peaks and valleys between 2000 and 2250 cm^{-1} are of the –CH stretching (of the saturated ring structure). The peaks at 1730 and 1650 cm^{-1} are due to bending of –OH groups. The 1350 and 1300 cm^{-1} responses are due to the $-CH_2$ bending vibrations.

5.4.1. Interactions of EC with water

The FTIR spectrum of wet EC film soaked in water shown in Fig. 5 can be compared with that of pure dry EC in Fig. 4. As expected, the peak at 3500 cm^{-1} is weakly affected, but the shift of its overtone at $\approx$1625 cm^{-1} towards the lower region is clearly due to absorption of water in the membrane. The –CH and –OH bending between 1300 and 1400 cm^{-1} are affected to some extent, but the ethoxy group vibrations are brought into focus at 2950 cm^{-1}. Otherwise, the spectrum remains largely unaffected indicating that EC film is hydrophilic but has somewhat fewer interactions with water molecules.

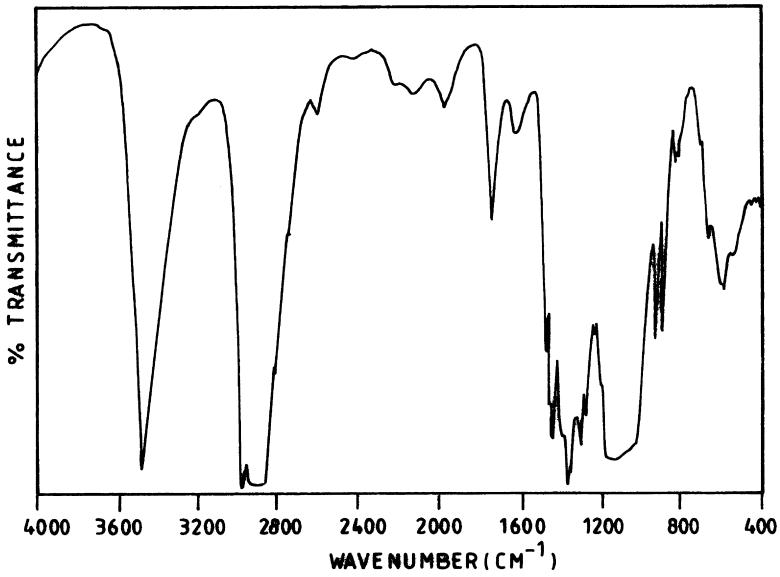

Fig. 5. FTIR spectrum of ethylcellulose soaked in water.

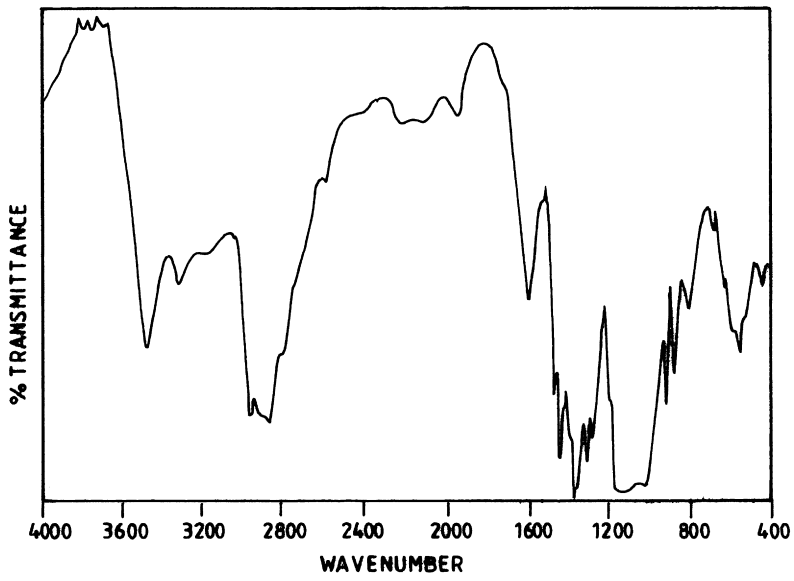

Fig. 6. FTIR spectrum of ethylcellulose soaked in monomethylhydrazine.

5.4.2. Interactions of EC with MMH

The locations or groups with which MMH has specific interactions are shown in Fig. 6. As in the case of hydrazine [26], MMH is interacting with the OH groups at 3500 cm^{-1}. This is confirmed by the decrease in the percentage of transmittance at this position. The decrease in wavenumber of appearance of OH groups clearly indicates the strong interaction of the group with MMH. A new peak at 3330 cm^{-1} corresponds to the stretching vibration of NH group. Leonard et al. [28], proposed an equation for identifying the symmetric and asymmetric $-NH_2$ stretching in a given compound. This can be written as

$$\gamma_s = 345.53 + 0.876\gamma_{as} \quad (18)$$

where γ is stretching vibrations of symmetric (s) and asymmetric (as) vibrations of NH_3 groups, respectively. If we assume that a peak at 3330 cm^{-1} is due to asymmetric vibrations, then the corresponding symmetric vibrations should appear around 3262 cm^{-1}. A small and broad peak at 3250 cm^{-1} clearly identified in Fig. 6 confirms that the response at 3330 cm^{-1} is due to the asymmetric stretching vibrations of $-NH_2$ group. In general the occurrence of this peak is around 3500 cm^{-1}. The decrease in 170 cm^{-1} peak strongly confirms the hydrogen bonding interactions between MMH and OH functional groups of EC. The same trend was also observed in symmetric stretching vibrations. The $-OC_2H_5$ ethoxy group at 3000 cm^{-1} has interactions with MMH as in the case of water and hydrazine

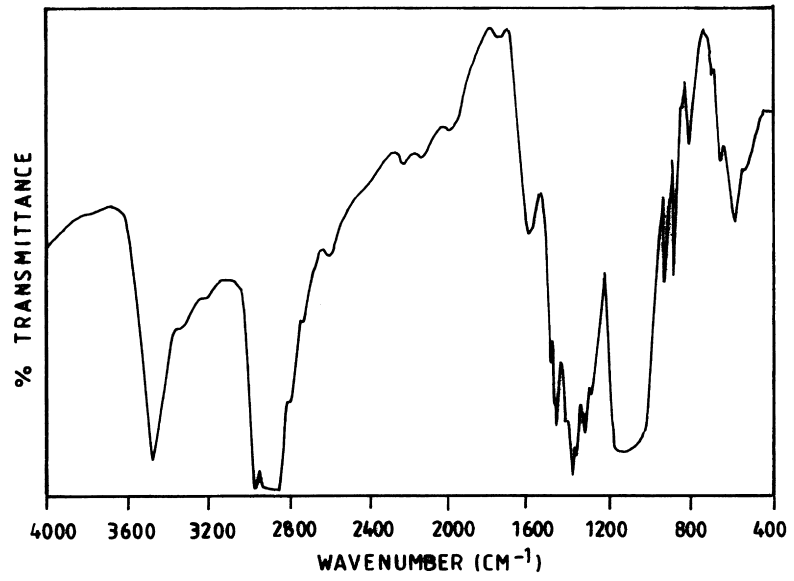

Fig. 7. FTIR spectrum of ethylcellulose soaked in hydrazine.

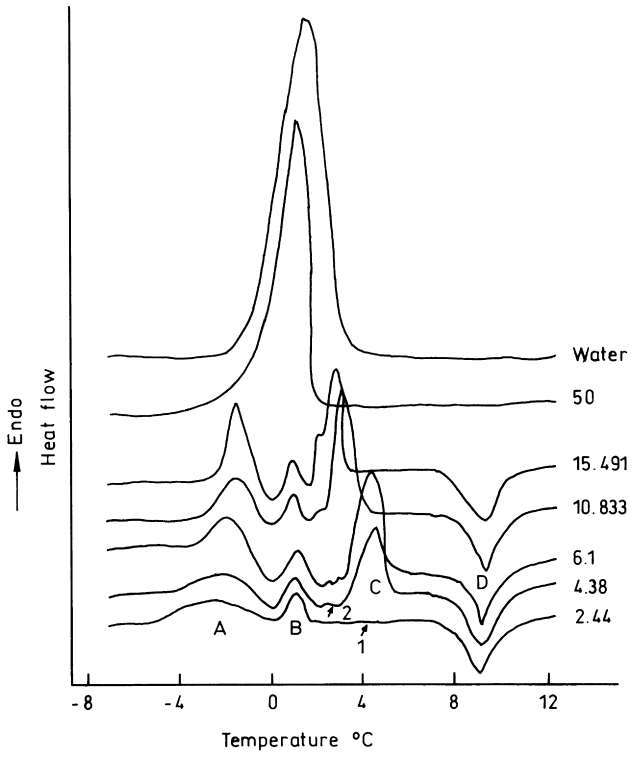

Fig. 8. DSC spectra of an EC–water system.

hydrate. A small peak appearing at 1622 cm^{-1} is due to the in-plane bending, corresponding to CH_2 scissoring, which is present in $CH_3–N_2H_3$ (MMH). The small but sharp peak at 1450 cm^{-1} is due to –NH– bending vibrations. A rather characteristic out-of-plane bending NH_2 peak corresponding to the CH_2 twisting is seen at 650 cm^{-1}.

When EC comes into contact with MMH the peak at 1800 cm^{-1} completely disappears. Moreover the peak at 1622 cm^{-1}, which becomes rather sharp again, indicates strong interaction of NH_2 with the functional groups present in the polymer. The corresponding peaks at 1622, 1360 and 700 cm^{-1} clearly indicate the presence of MMH and the positional shifts at 3330, 3500 and 1622 cm^{-1} proves the interaction of MMH with EC membrane. Both hydrazine and MMH have higher affinity for EC than water.

5.4.3. EC–hydrazine interactions

The locations of groups in which hydrazine has specific or strong interactions are quite obvious from a comparison of the spectrum of EC–hydrazine system in Fig. 7 with that of pure EC in Fig. 4. Hydrazine strongly interacts with OH groups at 3500 cm^{-1} and transmittance of the wet membrane is sharply reduced. The percent absorbency by OH vibrations becomes rather high and it increases with a decrease in wave number. A new peak is seen

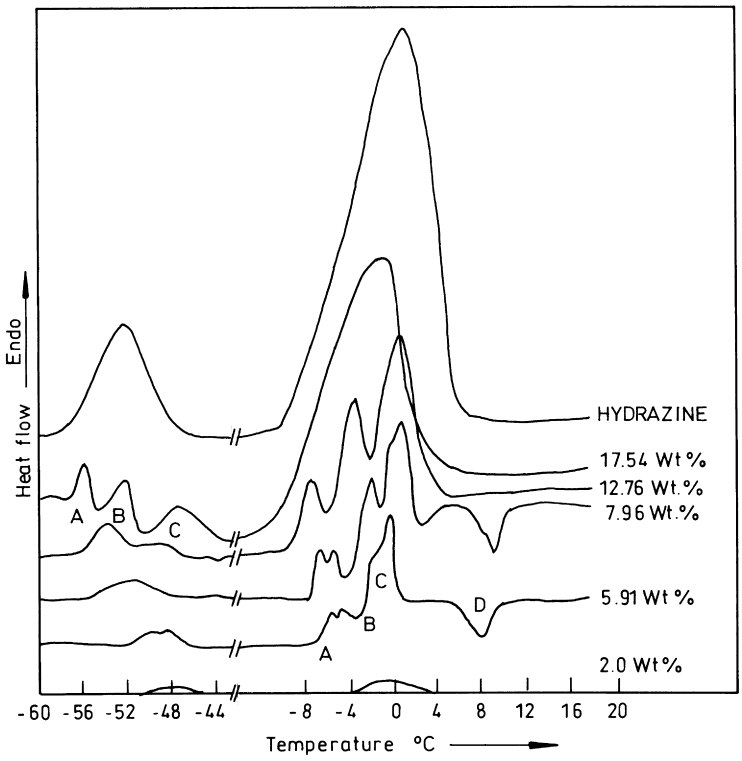

Fig. 9. DSC spectra of an EC–hydrazine system.

between 3300 and 3500 cm^{-1} corresponding to the free and associated forms of $-NH_2$ and –NH–. The former corresponds to that of free hydrazine molecules and the latter to hydrazine bonded with either water already present in polymer or the –CH of the cellulosic structure. The peak of associated –OH at 3200 cm^{-1} becomes rather sharp in the presence of hydrazine which was only a shoulder in the dry EC film or in the presence of water. The ethoxy $-OC_2H_5$ group at 3000 cm^{-1} has similar interactions with hydrazine as in the case of water. In the range 2250–3000 cm^{-1} corresponding to the –NH structure, the interaction (rather sharp) of EC with hydrazine is clearly visible. In the same range, water showed hardly any interactions with EC. The OH peak at 2050 cm^{-1} is also affected by hydrazine. However, both water and hydrazine show somewhat similar interactions and effects in the range 1200–1600 cm^{-1}. The peak at 1800 cm^{-1} has also rather sharpened indicating the possibility of CH···NH type bonding, thereby affecting the –CH bending. Amongst the two propellants, hydrazine interacts more strongly with EC than MMH which means than EC offers higher desorption resistance with hydrazine followed by MMH and then water.

5.5. DSC studies

DSC spectra of EC–water and EC–hydrazine systems are represented by Figs. 8 and 9, respectively [27]. Melting endotherms of the EC membrane were obtained for pure solvent concentrations ranging from about 2.55 to 50 wt%. DSC scans of only pure component liquids, without the membrane, were taken for reference. The values for each curve given at the right side of the figures specify the concentration of the solvent in the membrane. The letters A, B and C stand for the melt transitions of the three freezable states, i.e. *bound*, *interacting* (*absorbed*) and *free states* of the solvent in the membrane–solvent system. The *freezing free state* of the solvent (C) comprises the bulk solvent, which melts at higher temperatures than the solvent present in the membrane matrix, whereas the liquid present in the freezable interacting or adsorbed state (B) melts at lower temperatures than the bulk. The freezable bound state of the solvent arises due to diffusion of solvent molecules in the amorphous regions of the polymer and represents the region of least energy variation. Solvent present in this state melts at much lower temperatures than the other transitional states of B and C [29].

Quantitative estimation of each of the above three freezable states of solvent can be made from the melting curves by [30]

$$W_i = 100(Q_i/H_f) \tag{19}$$

where W_i is the percentage weight of the solvents in the individual peaks (A, B and C), Q_i is the total measured heat of transition under the peak and H_f is the enthalpy of solid–liquid transition of pure hydrazine or water.

There is also another solvent state, namely, the *non-freezable bound state*, which exists only at very low concentration of the solvent molecules in the polymer, say for example in the EC–water system if only one water molecule (H_2O) is available for two or three functional groups (OH) of EC. The amount of solvent present in this is given by

$$W_{nf} = W_T - (W_f + W_{fa} + W_{fb}) \tag{20}$$

where W_f, W_{fa} and W_{fb} are the percentage weights of are the percentage weights of solvent in the freezing states represented by C, B and A, respectively. W_T stands for the total solvent content in the membrane which is calculated as follows:

$$W_T = (W_w/W_d) \times 100 \tag{21}$$

where W_w and W_d are the weights of the solvent in the wet and dry EC membranes, respectively.

At very high concentrations of the liquids peaks corresponding to *free*, *bound* and *interacted* solvents have merged together resulting in a single peak similar to the one obtained for only pure solvent. This is because at higher concentrations, the membrane possesses a large quantity of unassociated bulk solvent besides smaller amounts of the three freezable ones due to which its melt transitions will be almost equal to the peaks corresponding to pure solvent. A new exothermic transitional peak represented by D in the figures, was observed for both pure water and pure hydrazine in the EC membrane which is attributed to the heat of dilution or mixing as the saturation of the polymer with solvent takes place [31].

A comparison of the DSC spectra in Figs. 8 and 9 shows that hydrazine has much more interaction and sorption in the EC membrane than water does. From the peaks of similar concentration of 6 wt% water in Fig. 8 and 5.91 wt% hydrazine in Fig. 9, it can be observed that much of the water is present in the bound state and little in free and interacting states, whereas the opposite trend was observed for hydrazine. In Fig. 8 the amounts of water in states A, B and C were found to be 2.5, 10.35 and 29.27 wt %, whereas in Fig. 9 the quantity of hydrazine was 5 wt% in state A and a combined weight of nearly 75% for the almost merged peaks B and C [20].

The thermal transition peak C indicating *free state* of solvent exists even below the equilibrium sorption level for hydrazine (7.96 wt %) whereas it is absent for water for concentrations below equilibrium percentage of sorption (3.4 wt % water in EC). The reason for this phenomenon may be explained based on the permeability coefficients of the components in the membrane that controls transport of solvent molecules across the membrane matrix during permeation as well as during the drying process. The relative permeability or selectivity (α) is collected from the individual permeabilities of water (P_1) and hydrazine (P_2) as follows:

$$\alpha = P_1/P_2 = (S_1 \times S_2)/(S_2 \times D_2)$$

From pervaporation experiments the value of α was found to be 3.94 with respect to water. However since $S_1 < S_2$ and $\alpha > 1$, D_1 must be greater than D_2. Kinetic sorption experiments were performed by plotting reduced sorption curves [32] and diffusion of water through the EC membrane ($D_1 = 2.57 \times 10^{-8}$ cm^2/s) was proved to be greater than that of hydrazine ($D_2 = 0.28 \times 10^{-8}$ cm^2/s). Hence the smaller diffusivity value of hydrazine in the membrane ensures that it moves relatively slowly from the bulk solution and exists at the surface layers of the film, which explains the appearance of *free state* of hydrazine below the equilibrium sorption concentration.

In Fig. 9 a well-resolved interacting peak (B) obtained for 17.54 wt% hydrazine concentration, can be seen. At this concentration, the membrane was found to contain 0.2869 mg of interacting hydrazine which is much higher than the interacting water content (0.0342 mg) for the membrane having 15.49 wt% total concentration as shown in Fig. 8 [27]. This means that hydrazine is greatly influencing the functional groups of EC thereby providing channels for water molecules to diffuse more freely.

In Fig. 9, a small peak appears at sub-ambient temperatures of −58 to −50°C owing to the melting transition of hydrazine coupled with trace quantities (<4%) of water. At low concentrations this peak is very broad and becomes sharper with increasing hydrazine concentration and finally splits into three peaks at 47.19 wt% concentration of the liquid propellant due to the deformation of *bound*, *interacting* and *free states* at sub-ambient temperatures. Quantitative evaluation of each these peaks at such low temperatures is not possible. Similarly quantitative estimations pertaining to DSC spectra of hydrazine hydrate in EC cannot be carried out because at the state of equilibrium sorption, the actual melting temperatures of bulk water and hydrazine are 0 and 2°C, respectively, and at this temperature range the transitions of hydrazine hydrate–EC system also occur thus making characterisation of individual peaks very difficult.

MMH and its hydrates melt at very low temperatures (below −60°C) at which some of the other transitions, possibly of alpha, beta etc., merge with the melting endotherms of membrane–solvent interactions and therefore DSC spectra for these systems could not be obtained.

6. Conclusions

Diffusion through membranes and desorption resistance of the liquid species are the two most important factors that govern the selectivity in pervaporation. Interactions, sorption and diffusion are the key factors that affect the desorption resistance and membrane resistance. The desorption parameters pertaining to ethylcellulose membranes were estimated for water, hydrazine and MMH by pervaporation experiments. Due to higher interaction capability, which was confirmed by FTIR and DSC analysis, hydrazine offers higher desorption resistance. Smaller Hansen and Flory–Huggins interaction parameters are the main reasons for the higher percent of sorption of MMH with EC than the other two liquids. Thus, MMH will have the lowest diffusion coefficient through the membrane. Smaller diffusion coefficients of MMH in EC show better selectivity for the MMH–water system than hydrazine–water. Results of the pervaporation studies proved the same. In brief, the interactions of liquids with the polymer functional groups will influence the desorption resistance, whereas the diffusion and sorption values demonstrate the membrane resistance.

Acknowledgements

The authors thank the Vikram Sarabhai Space Center-Indian Space Research Organisation (VSSC-ISRO), India, for funding the studies under their ‘RESPOND’ program.

References

[1] Seak DR, Kaug SG, Hwang ST. J Membr Sci 1987;33:71.
[2] Mulder MHV, Kruitz F, Smolders CA. J Membr Sci 1982;11:349.
[3] Blume I, Wijmans JG, Baker RW. J Membr Sci 1990;49:253.
[4] Ishihara K, Matsui K. J. Appl Polym Sci 1987;34:437.
[5] Hirotsu T, Tshimura K, Mizoguchi K, Nakmura E. J Appl Polym Sci 1988;36:1717.
[6] Binning RC, Lee RJ, Jenning JF, Martin CE. Ind Inorg Chem 1961;53:45.
[7] Coo CY. Adv Petrol Chem Refining 1963;6:73.
[8] Brun JP, Larchet C, Bulvestre G, Auclair B. J Membr Sci 1985;5:55.
[9] Nguyen QT. Ken Nobe. J Membr Sci 1987;30:11.
[10] Huang RYM, Fels M. Chem Engng Properties Symposia Ser 1969;65:52.
[11] Hugging J. Chem Engng News, Am Chem Soc 1990;68:22.
[12] Lee CH. J Appl Polym Sci 1975;19:83.
[13] Nijhuis HH, Mulder MHV, Smolders CA. J Membr Sci 1991;61:99.
[14] Cote J, Lipski C. Proceedings of the Third International Conference on Pervaporation Process in the Chemical Industry. Nancy, France, September, 19–22, 1988. p. 449.
[15] Bode E. Proceedings of the Third International Conference on Pervaporation Processes in the Chemical Industry. Ft Lauderdale, Florida, December 3–7, 1989. p. 103.
[16] Raghunath B, Hwang ST. J Membr Sci 1992;61:99.
[17] Bode E, Busse M, Ruthenberg K. J Membr Sci 1993;77:69.
[18] Rigbi Z. Polymer 1978;1:1229.
[19] Brun JP, Larchet C, Melet M, Bulvestre G. J Membr Sci 1985;23:257.
[20] Ravindra R, Sridhar S, Khan AA. J Polym Sci, Polym Phys Ed 1999; in press.
[21] Ravindra R, Khan AA, Kameswara Rao A. Proceedings of IInd International Conference and Exhibit of High Energy Materials. IIT, Chennai, India, 8–10 December, 1998. p. 212–16
[22] Scott DW. J Am Chem Soc 1949;71:2293.
[23] Agarwal HP, Agarwal BB. Indian J Chem 1979;17A:428.
[24] Aston JG. J Am Chem Soc 1951;73:1939.
[25] Aerojet General Corp., Handbook of properties of UDMH and MMH, Aerojet Gen Corp Report. May, 1958.
[26] Ravindra R, Krovvidi KR, Khan AA, Kameswara Rao A. Macromolecules 1997;30:3288.
[27] Ravindra R, Krovvidi KR, Khan AA, Kameswara Rao A. Polymer 1999;40:1159.

[28] Leonard NJ, Owens FH. J Am Chem Soc 1958;80:6039.
[29] Taniguchi T, Horigome S. J Appl Polym Sci 1975;19:2743.
[30] Hodge RM, Graham HE, Simon GP. Polymer 1996;37:1371.
[31] Barrer RM, Barrie JA, Slater J. J Polym Sci 1958;27:177.
[32] Comyn J, editor. Polymer permeability. Amsterdam: Elsevier, 1985. p. 26.
[33] Schmidt AB. Hydrazine and its derivatives. New York: Wiley, 1984. Chapter 2, p. 138–45.
[34] Bandrup J, Immergut EH, editors. Polymer handbook. New York: Wiley, 1975. Chap 4.
[35] Barton AFM, editor. CRC handbook of solubility parameters and other cohesive parameters. Boca Raton, FL: CRC Press, 1983.
[36] Okuno H, Nishida T, Uragami T. J Polym Sci, Polym Phys 1995;33:299.